Theor Appl Climatol (2016) 126:313–321
DOI 10.1007/s00704-015-1587-7

ORIGINAL PAPER

Role of delayed deep convection in the Madden-Julian oscillation

Fei Liu[1] · **Zaoyang Chen**[1] · **Gang Huang**[2,3]

Received: 2 December 2014 / Accepted: 21 July 2015 / Published online: 4 August 2015

Abstract The power spectrum of Madden-Julian oscillation (MJO) has a peculiar dispersion relation and is well separated from the convectively coupled equatorial waves (CCEWs). The authors present a theoretical model coupling the equatorial Rossby and Kelvin waves to understand this spectral feature of MJO. In this model, a delay process for triggering the deep convection from the additional planetary boundary layer (PBL) pumped moisture is implemented. This model has a moist Kelvin wave-like dispersion relation, and short waves grow fast when all moisture pumped by the PBL excites the deep convection instantly. When the moisture pumped by the PBL is delayed to stay in the lower troposphere for a time scale on the order of a day before triggering the deep convection, this model simulates a MJO-like mode, for which three features of the MJO, the peculiar dispersion relation, the horizontal quadrupole-vortex structure, and longest waves having maximum growth rate, have been simulated. Both moist Kelvin wave-like mode and MJO-like mode are simulated simultaneously when part of the deep convection is delayed, where the strong instability occurs at low-frequency long wavelength for the MJO-like mode and at high-frequency short wavelength for the moist Kelvin wave-like mode. These results suggest the importance of the delay process of deep convection in simulating the MJO.

✉ Gang Huang
hg@mail.iap.ac.cn

[1] Earth System Modeling Center and Climate Dynamics Research Center, Nanjing University of Information Science and Technology, Nanjing 210044, China

[2] State Key Laboratory of Numerical Modeling for Atmospheric Sciences and Geophysical Fluid Dynamics (LASG), Institute of Atmospheric Physics, Chinese Academy of Sciences, Beijing 100029, China

[3] Joint Center for Global Change Studies (JCGCS), Beijing 100875, China

1 Introduction

The Madden-Julian oscillation (MJO), named after its discoverers, is one of the most important modes in the tropical atmosphere (Madden and Julian 1971, 1972, 1994). The MJO features an equatorially trapped planetary-scale baroclinic circulation cell that propagates eastward slowly (about 5 m s^{-1}) in the eastern hemisphere (Knutson and Weickmann 1987; Wang and Rui 1990; Hendon and Salby 1994; Maloney and Hartmann 1998; Kiladis et al. 2005; Zhang 2005). Whereas it prevails in the equatorial region, the MJO has significant impacts on a wide variety of climate phenomena across different spatial and temporal scales (Zhang 2005; Zhou and Miller 2005; Mori and Watanabe 2008).

In observations, the power spectrum of MJO is distinct from all convectively coupled equatorial waves (CCEWs) (Wheeler and Kiladis 1999; Kiladis et al. 2005; Zhang 2005; Kiladis et al. 2009). For the eastward-propagating signals, the moist Kelvin waves have a linear dispersion relation between the frequency and wavenumber, and its power spectrum is maximum at the wavenumbers from 4 through 8. The MJO is very different, which power spectrum is maximum on the planetary scale and has a peculiar dispersion relation, for which the frequency is wavenumber independent.

When located over the equatorial Indian Ocean and the western Pacific, the MJO has a quadrupole-vortex horizontal structure, and it can be treated as a coupling of equatorial Rossby wave and Kelvin wave (Rui and Wang 1990; Hendon and Salby 1994). In the frictional wave dynamics, the

planetary boundary layer (PBL) pumps additional moisture in front of the MJO convective center to support the deep convection, and the eastward-propagating mode has the strongest instability at the planetary scale when longwave approximation was used in the PBL (Wang and Rui 1990). The moisture pumped by the PBL, however, was parameterized as the deep convective heating directly, and this frictional wave dynamics only simulates the moist Kelvin wave-like dispersion relation, for which the frequency increases linearly with increasing wavenumber. This is dramatically different from the peculiar dispersion relation of MJO.

Recently, the effects of the moisture feedback were found to be important to simulate the MJO dispersion relation. A "moisture mode" isolating the moisture feedback was presented by Sobel and Maloney (Sobel and Maloney 2012, 2013), in which the moisture perturbation is the only prognostic variable and the instability comes from the thermodynamic feedback. In their works, the wind-evaporation feedbacks were found to induce westward propagation in an easterly mean low-level flow, while zonal advection, modulation of synoptic eddy drying by the MJO-scale wind perturbations, and frictional convergence all help in destabilizing the easterlies and favors the eastward propagation. In their work, the simulated eastward propagation is well separated from the CCEWs. Since no wave dynamics was included, the eastward propagation of the "moisture mode" is too slow compared to the observation. Considering both wave dynamics and moisture feedback, Majda and Stehmann (Majda and Stechmann 2009) proposed a MJO skeleton model, in which a neutral mode with slow eastward propagation was simulated along with a peculiar dispersion relation $\partial\sigma/\partial k = 0$, where σ and k are frequency and wavenumber, respectively. The PBL moisture convergence was found to provide an instability source for this slow eastward propagation (Liu and Wang 2012a).

Whereas these theories all provide some insight into the mechanism of MJO, it is still not clear what the critical process is for simulating the peculiar dispersion of the MJO and why the MJO is well separated from the CCEWs, especially from the moist Kelvin waves. In the present study, we intend to answer these questions by using a simple theoretical model, in which the delay process of the deep convection triggered from the PBL pumped moisture is parameterized.

2 The frictional wave dynamics with delayed deep convection

The large-scale MJO involves semi-geostrophic, low-frequency equatorial Kelvin wave and Rossby wave. Based on the important interaction of the equatorial waves, boundary layer dynamics and collective effects of convective heating (Wang 1988; Zhang 2005), Wang and Rui (1990) built up a frictionally coupled Kelvin-Rossby wave model that includes PBL moisture convergence jointly generated by the Kelvin and Rossby waves. In this model, the instability mainly comes from the PBL moisture convergence, which can be obtained from the steady PBL model (Wang and Li 1994; Liu and Wang 2012a).

Without additional moisture source from the PBL, the troposphere is stable for the moist Kelvin wave and moist Rossby wave (Wang 1988), and the moist Kelvin and Rossby waves should propagate eastward and westward separately. The Rossby and Kelvin waves both excite upward Ekman pumping to their east sides (Wang and Rui 1990), thus the additional moisture coming from the PBL will support the growth of the convection, which couples the Rossby and Kelvin waves and results in an eastward-propagating Gill-like pattern.

To obtain the nondimensional equations, we take $C = 50$ ms^{-1} (the lowest speed of internal gravity waves) as the reference speed, and the characteristic temporal and spatial scales as $\sqrt{1/C\beta} = 8.5$ h and $\sqrt{C/\beta} = 1500$km, respectively, where $\beta = 2.3 \times 10^{-11} m^{-1}s^{-1}$ representing the leading order curvature effect of the Earth at the equator. Assuming that the PBL motion is forced by the pressure anomalies in the lower troposphere, the nondimensional PBL moisture convergence can be written as:

$$q_{ek} = r_b(\mathrm{SST}-9.18)\frac{H_b}{H_T}\left[d_1\partial_{xx}\phi + d_1\partial_{yy}\phi + d_2\partial_x\phi + d_3\partial_y\phi\right] \quad (1)$$

where ϕ is the lower tropospheric pressure anomaly. The PBL coefficients are $d_1 = E/\left(E^2+y^2\right)$, $d_2 = -\left(E^2-y^2\right)/\left(E^2+y^2\right)^2$, and $d_3 = -2Ey/\left(E^2+y^2\right)^2$. The standard PBL coefficient is $r_b = 0.06$ (Liu and Wang 2012a). SST is the sea surface temperature (SST), and a temperature of 30 °C has been used at the equator. The PBL depth $H_b = 1$ km and troposphere depth scale is $H_T = 16/\pi = 5.1$ km (Majda and Biello 2004). The frictional scale of the PBL, E, is selected to represent a damping time scale of one-third day. The nondimensional frictional wave dynamics can be written as (Wang and Rui 1990):

$$\begin{aligned} &\partial_t u - y\,v + \partial_x\phi = 0, \\ &y\,u + \partial_y\phi = 0, \\ &\partial_t\phi + \left(1-\tilde{Q}_f\right)\left(\partial_x u + \partial_y v\right) = -F, \end{aligned} \quad (2)$$

where u and v are the zonal and meridional velocities, respectively, and F is the diabatic heating caused by the additional moisture pumped by the PBL. The nondimensional magnitude of vertical gradient of the background moisture $\tilde{Q}_f$ is taken to be 0.95 above a warm SST with a value of 30 °C (Liu and Wang 2012a).

In the frictional wave dynamics (Wang and Rui 1990), the moisture pumped by the PBL is parameterized as the deep

convective heating directly, which means that the moisture convergence from the PBL will excite the deep convection instantly without any delay. While in the framework including moisture process, the PBL moisture convergence is parameterized into *moisture tendency*, and a phase lag between the deep convection and PBL moisture convergence exists. This phase lag was also introduced in the frictional MJO skeleton model (Majda and Stechmann 2009; Liu and Wang 2012a). Here, we assume that a part of the moisture pumped by the PBL, i.e., αq_{ek}, should be delayed before triggering the deep convection with an adjustment time of τ, and the remaining part $(1-\alpha)q_{ek}$ will excite the deep convection instantly; thus, the total convective heating coming from the PBL moisture convergence is

$$F = F_D + F_S, \tag{3}$$

where

$$\begin{aligned} F_D &= (1-\alpha)q_{ek}, \\ \partial_t F_S &= \frac{\alpha q_{ek}}{\tau}. \end{aligned} \tag{4}$$

In the above equations, F_D denotes the deep convective heating coming from the PBL moisture convergence instantly, and F_S is the delayed part. The tendency of F_S is assumed to be proportional to the PBL moisture convergence, which means that the positive (negative) PBL moisture convergence anomalies create a *tendency* to enhance (decrease) the deep convection. In the observation, the deep convection of the MJO usually lags its leading PBL moisture convergence by a time scale on an order of 1 day (Mapes et al. 2006; Hsu and Li 2012; Jiang et al. 2015), and a time scale of 1 day is used here for the delay time τ. The sensitivity experiments for this critical parameter will be reported in the next section.

Equations (1–4) are a set of linear partial differential equations, for which the eigenvalue problem can be readily solved. For the zonally propagating planetary waves, we assume which have a structure of e^{i} $(kx-\sigma t)$. The phase speed and growth rate are defined by $\mathrm{Re}(\sigma)/k$ and $\mathrm{Im}(\sigma)$, respectively. After projected (1–4) onto the frequency-wavenumber space, the eigenvalues and eigenvectors can be calculated through matrix inversion corresponding to each wavenumber. Because of the longwave approximation in the troposphere, only Kelvin and Rossby waves are kept, and their lowest modes can be represented by the lowest three meridional modes of the meridional expansion of parabolic cylinder functions. The Rossby and Kelvin waves can be represented by using $N \leq 3$, and sensitivity experiments indicate that a higher N does not affect the results (not shown). In the observation, the climatological mean SST is usually maximum at the equator and decays poleward (Kang et al. 2013; Liu et al. 2014); thus, only the lowest meridional mode (lowest mode of parabolic cylinder functions) of the associated $\tilde{Q}_f$ and *SST* is used.

In order to see the relative contributions of the equatorial Kelvin and Rossby waves to these linear waves, we simply define a Rossby-Kelvin ratio by the rate of the maximum geopotential anomalies between the subtropical region (15°–25°N) and equatorial (5°S–5°N) region.

3 Model results

Figure 1 shows the frequency and growth rate for different processes. When the moisture pumped by the PBL is not delayed ($\alpha = 0$), that is, all of it excites the deep convection instantly, the model has a dispersion relation in which the frequency increases linearly with the increasing wavenumber. This dispersion relation is similar with that of the moist Kelvin waves. The horizontal structure of this mode is also dominated by the Kelvin waves, in which the Rossby component is very weak, and the Rossby-Kelvin ratio is only 0.1. In this solution, all modes are unstable, among which shorter waves have stronger instabilities. The longwave approximation in the PBL can suppress the short waves and solve this "ultraviolet catastrophe" problem (Wang and Rui 1990).

When all the moisture pumped by the PBL is parameterized to be delayed for some hours (with a time scale of 1 day) before triggering the deep convection ($\alpha = 1$; Fig. 1b), a *new MJO-like* solution, which has a wavelength-independent dispersion relation, is introduced. The introduction of this new solution can be shown by taking the Kelvin wave as an example. The formula for the frequency of the frictional moist Kelvin waves is a quadratic equation; only one solution exists for the eastward-propagating mode and another solution exists for the westward propagating mode (Wang 1988). When the delay process is included, a formula for the intraseasonal oscillation frequency of this model can be obtained by considering an even simpler case of flow above the equator. In this case, v and y are set to zero, and the meridional derivatives are ignored. We take the PBL longwave approximation and ignore the zonal derivatives in the PBL

$$q_{ek} = r_b(\mathrm{SST}-9.18)\frac{H_b}{H_T}d_1\phi_{yy}, \tag{5}$$

and the formula for the frequency can be written as:

$$\sigma^3 - \left(1-\tilde{Q}_f\right)k^2\sigma - d_1\frac{\tilde{Q}_b}{\tau}k = 0, \tag{6}$$

which is a cubic equation. The coefficient $\tilde{Q}_b = -r_b(SST-9.18)\frac{H_b}{H_T}$. A new solution is introduced in Eq. (6).

It is interesting that, for this new solution, the longest wave has the strongest instability, which can be explained by the wavelength-dependent delay process (Fig. 2): The short

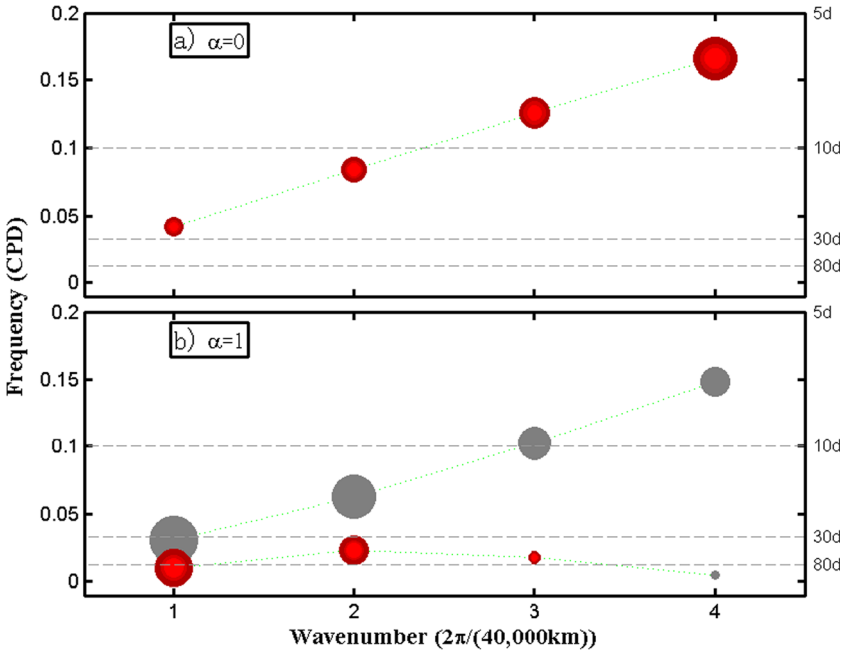

Fig. 1 Linear wave oscillation frequency as functions of wavenumber for eastward-propagating modes. Two experiments are carried out, in which **a** no moisture pumped by the PBL is delayed ($\alpha = 0$) and **b** all moisture pumped by the PBL is delayed ($\alpha = 1$) before triggering the deep convection. *Red* and *gray* denote unstable and damped modes, respectively. Marker diameter corresponding linearly to growth rate and the maximum growth rate is 0.3 day^{-1}

waves have a large phase lag between the deep convection and PBL moisture convergence. As a result, the available potential energy is small for short waves and may even become negative for wavenumber 4 (not shown). The wavenumber-dependent relation between deep convection and PBL moisture convergence can be explained by Eq. (4): the phase lag between deep convection and PBL moisture convergence is determined by, and inversely proportional to, the magnitude of the frequency σ. From Fig. 1b, we can see that the frequency is small for short waves; thus, the phase lag is large for short waves. From Eq. (6), the first-order term and zero-order term with respect to the frequency are proportional to k^2 and k, respectively, which means that two solutions are proportional to k associated with the eastward/westward linear dispersion relations and the third solution is inversely proportional to k associated with the peculiar dispersion relation.

This conclusion about wavelength-dependent delay process and associated longwave selection is important to understand the MJO's scale selection. This conclusion, however, is based on this simple theoretical model, and it needs further works on observation analysis to test this finding in the future works.

The successful representation of the MJO dispersion relation in this model prompted us to explain why the delay process of deep convection can slow down the eastward propagation. As noted in previous work (Wang 1988), the troposphere is usually stable for the wind convergence, and the additional diabatic heating coming from the PBL moisture convergence is an important instability source. Without the delay process of deep convection, the additional middle-tropospheric diabatic heating, coming from the PBL moisture convergence, is in phase with the Ekman pumping (Fig. 3a), which leads the tropospheric moisture convergence and induces fast eastward propagation. The model with delay processes has behavior that can be qualitatively different from that without delay processes (Fig. 3b), and the additional middle-tropospheric diabatic heating is collocated with the tropospheric convergence and lags the Ekman pumping. This additional middle-tropospheric diabatic heating should enhance the wind convergence and slow down the eastward propagation.

It is interesting that the horizontal quadrupole-vortex structure is also simulated associated with the slow eastward propagation of the MJO-like mode (Fig. 3b). This horizontal quadrupole-vortex structure, with a stronger Rossby component, was also simulated by the skeleton model when the delay process was included (Majda and Stechmann 2009; Liu and Wang 2012a, 2013a).

This slowdown of eastward propagation caused by a delay process of deep convection was also shown by the "moisture mode" theory (Sobel and Maloney 2012, 2013). In their works, a very slow eastward propagation, which is well separated from the CCEWs, was simulated with a convective time scale on the order of a day. Since no wave dynamics was included there, the simulated eastward propagation is much slower than observation.

For different delay time, the first eastward-propagating solutions are always strong damping modes having a moist Kelvin wave-like dispersion relation (not shown). The second solution introduced by the delay process is very different, and Fig. 4 shows that this new MJO-like solution is very sensitive to the delay time τ. For this second solution, the model presents stationary modes at some wavenumbers. These stationary modes are very different from the propagating ones, and their pressure and PBL convergence anomalies are

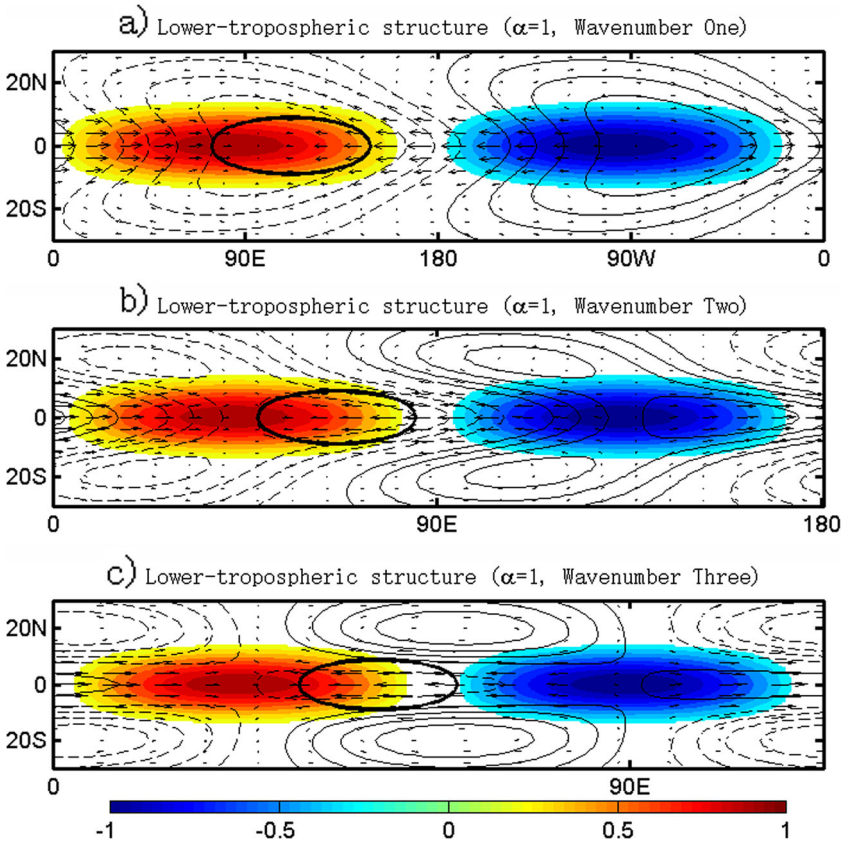

Fig. 2 Horizontal structures of normalized precipitation (*shading*), winds (*vectors*), geopotential (*thin contours*), and upward Ekman pumping (*thick contour*) for **a** the unstable wavenumber 1, **b** the unstable wavenumber 2, and **c** the unstable wavenumber 3 when all moisture pumped by the PBL is delayed ($\alpha = 1$). Contour interval is 0.2, and positive (*negative*) values are indicated by *solid* (*dashed*) *contours*. Only upward Ekman pumping with a value of 0.8 is contoured. To show their relative phase relationship, only one cycle has been drawn for different wavenumbers

zero, which means that a balance between the wind convergence and diabatic heating exists and the PBL process is not included. As we focus on the role of the PBL moisture convergence, we delete this stationary solution in which the PBL tropospheric circulation and PBL process are not coupled.

When the delay process is short that represents the moisture pumped by the PBL will stay in the lower troposphere for only few hours, this new solution only exist since wavenumber 4, in which only wavenumber 4 is unstable and this new solution does not exist for the long waves. When the delay process is

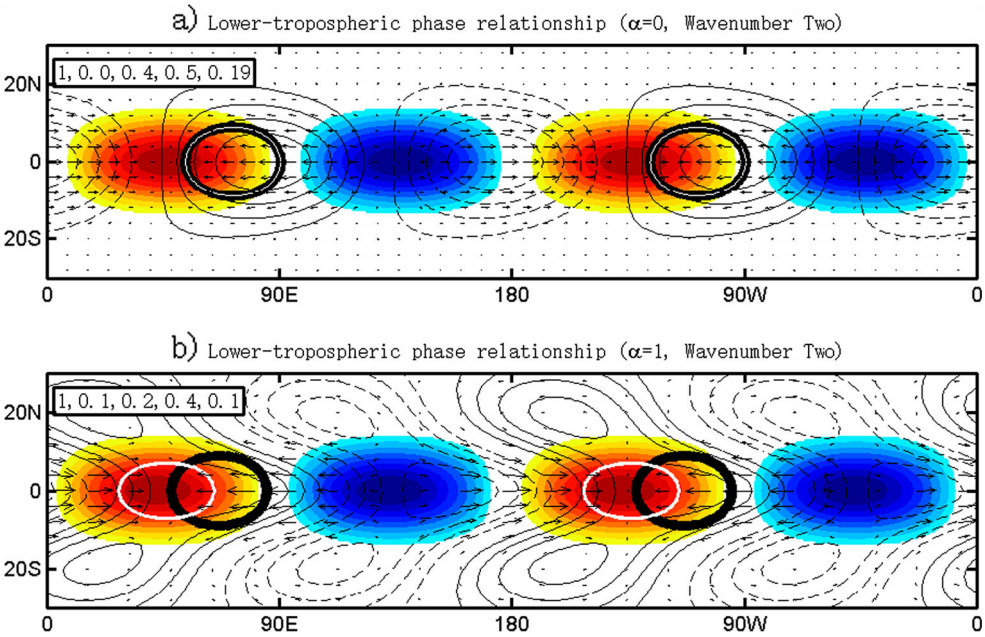

Fig. 3 Horizontal structures of normalized precipitation (*shading*), winds (*vectors*), geopotential (*thin contours*), and upward Ekman pumping (*thick contour*) for the unstable wavenumber 2 in the experiments **a** with and **b** without the delay processes. The *white lines* denote the diabatic heating F_S in (**a**) and F_D in (**b**), respectively. Contour interval is 0.2, and positive (*negative*) values are indicated by *solid* (*dashed*) *contours*. Only upward Ekman pumping with a value of 0.8 is contoured

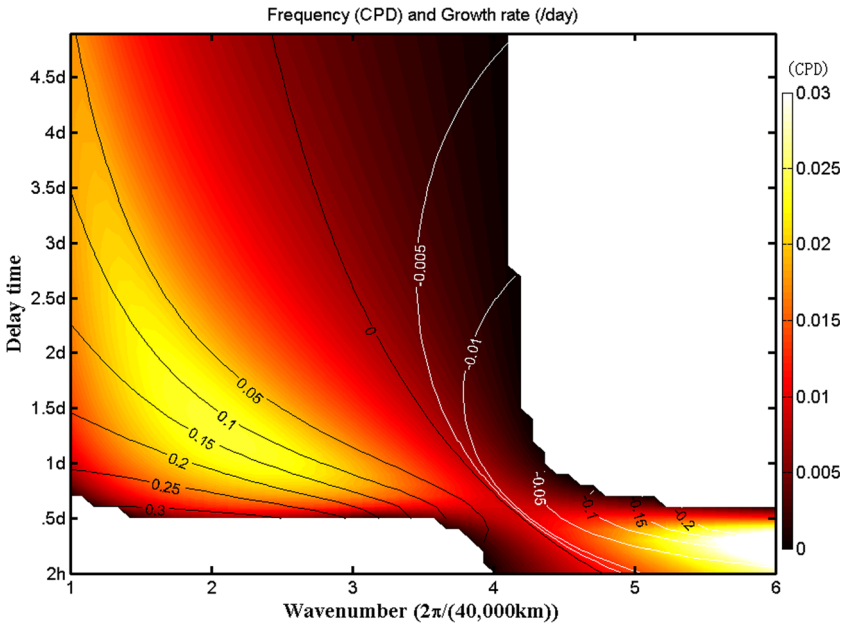

Fig. 4 MJO-like solution associated with the eastward-propagating mode for different delay time scales. Frequency (*shading*) and growth rate (*contour*) as functions of wavenumber and delay time are shown for the calculation when all moisture pumped by the PBL is delayed ($\alpha = 1$). Positive and negative values are denoted by *black* and *white* contours, respectively. Over the blank regions, the MJO-like solutions do not exist

long, namely, the moisture pumped by the PBL will stay in the lower troposphere for some hours before triggering the deep convection, this new solution exists on the planetary scale having an oscillation period of 30–90 days, while this new solution does not exist for short waves.

Sensitivity experiments with respect to the PBL coefficient $\tilde{Q}_b$, the PBL damping E, and the vertical gradient of mean moisture $\tilde{Q}_f$ all show this new solution drastically changes near wavenumber 4. For the frictional Kelvin waves with delay process of deep convection, this new eastward-propagating modes exist for all wavenumbers (figure not shown), which means that the drastic change in this new solution may be caused by the coupling of Rossby waves, Kelvin waves, and PBL moisture convergence. The frequency of this MJO-like mode is maximum at wavenumbers 2 and 3 when the delay time is about 1–2 days. In Eq. (6), the frequency is determined by the wavenumber and other parameters such as the moist static instability and delay time. The explanation may be of interest in future studies but is not considered here.

To understand why the MJO only propagates eastward, our explanation which based on these theoretical results are in broad agreement with the observation analysis (Hsu and Li 2012) and GCM simulations (Hsu et al. 2014); the eastward propagation of the MJO is caused by the moisture asymmetry. Because of the intrinsic character of the eastward-propagating Kelvin waves, the low-level negative pressure anomalies will excite upward Ekman pumping to the east side of the convective center, which tends to moisten the lower troposphere and generates this moisture asymmetry, i.e., positive/negative moisture anomaly in front of/behind the convective center. This moisture asymmetry will induce the eastward propagation of the MJO-like mode.

In observations, the congestus clouds were observed to prevail in front of the convective center of the MJO (Benedict and Randall 2007; Zhang and Song 2009; Del Genio et al. 2012), where the fast eastward-propagating Kelvin waves coupled with deep convection were also observed (Roundy 2008). These observations mean that some of the moisture coming from the PBL Ekman pumping becomes the deep convection instantly relative to the MJO, while some of them tends to form the shallow congestus cloud that accumulates the moisture to the eruption of deep convection (Khouider and Majda 2006, 2007). To mimic this process, we make a simple assumption that only a half part of the PBL moisture convergence is delayed (Fig. 5). This model gives both unstable high-frequency short waves and unstable low-frequency planetary-scale waves, associated with the first and second solutions, respectively. The first solution has a moist Kelvin wave-like dispersion relation, and the short waves grow fast. The second MJO-like solution has a peculiar dispersion relation and the planetary-scale waves are most unstable. This result means that the delay process will select the planetary-scale waves to have the strong instability, while the frictional instability without delay process will select the high-frequency short waves. This simulated power spectrum in Fig. 5 mimics the observed power spectrum of the MJO and moist Kelvin waves well (Kiladis et al. 2009).

Figure 6 shows the horizontal structures of the unstable wavenumber 4 and wavenumber 1 in Fig. 5. The horizontal structure of the unstable short wave is dominated by the equatorial moist Kelvin waves, and the Rossby component is very weak, represented by a small Rossby-Kelvin ratio with a value of 0.2. The unstable wavenumber 1 shows a coupled Rossby-Kelvin structure with a strong Rossby component, and the Rossby-Kelvin ratio is 0.6.

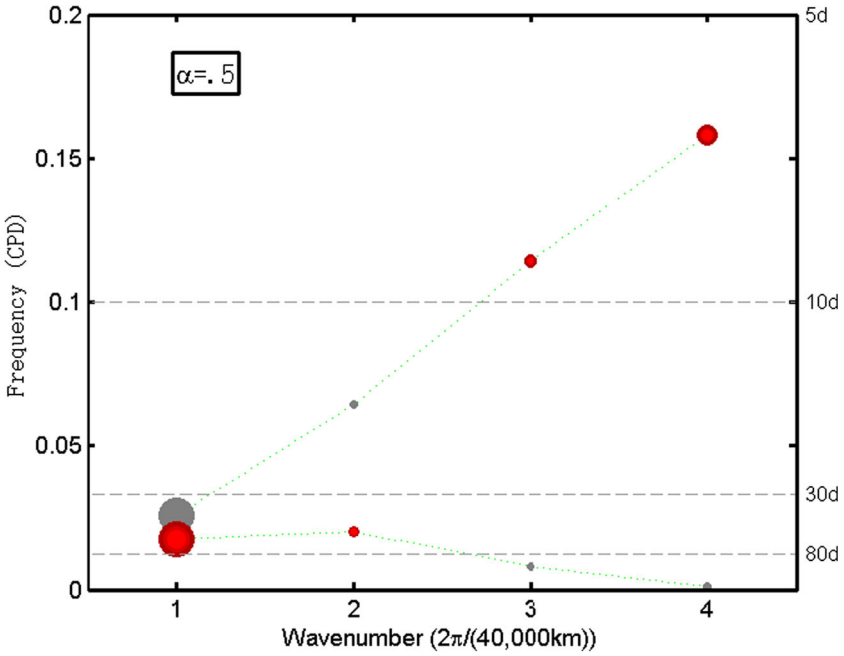

Fig. 5 Same as in Fig. 1, except for the case when half of the moisture pumped by the PBL is delayed ($\alpha = 0.5$)

4 Concluding remarks

The authors present a simple theoretical model, including the planetary boundary layer (PBL) moisture convergence and the delay process of deep convection, to simulate the unstable low-frequency Madden-Julian oscillation (MJO)-like mode and unstable high-frequency moist Kelvin wave-like mode simultaneously, which is in broad agreement with the observations (Kiladis et al. 2009). The delay process of deep convection is responsible for the selection of planetary-scale waves having the strongest instability and for the separation of MJO-like mode from the convectively coupled equatorial waves (CCEWs).

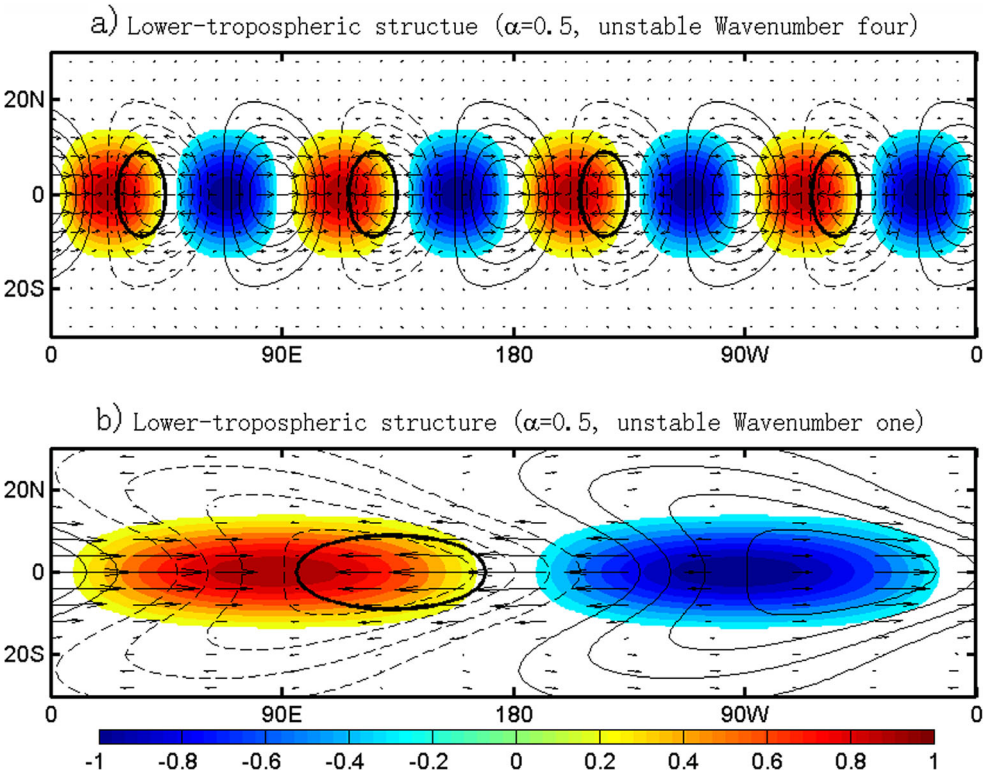

Fig. 6 Same as in Fig. 2, except for **a** the unstable wavenumber 4 and **b** the unstable wavenumber 1 in the calculation when half of the moisture pumped by the PBL is delayed ($\alpha = 0.5$)

The frictional wave dynamics without the delay process will select the short waves to have the strongest instability.

The delay process of the deep convection is also found in the observation and in the general circulation models (GCMs) simulation for the MJO. In recent model analysis (Jiang et al. 2015), the GCMs with good MJO simulations all show significant delay of deep convection, and an upward vertical and westward tilt exists. In front of the deep convection of the MJO, the congestus clouds were observed to prevail (Benedict and Randall 2007; Zhang and Song 2009; Del Genio et al. 2012), which accumulates the moisture pumped from the PBL and delays the eruption of deep convection (Khouider and Majda 2006, 2007). Thus, our theoretical results demonstrate that proper simulation of the moisture accumulation and the delay process of deep convection are important for adequately simulating the MJO in the GCMs.

In this theoretical model, the propagation mechanism relies on the role of intraseasonal pressure anomalies near the equator (Wang and Rui 1990; Salby and Hendon 1994). In the tropics, there are also a number of works based on the weak temperature gradient (WTG) approximation against these strong pressure asymmetry (Sobel et al. 2001; Sobel and Maloney 2012, 2013). Examination of this PBL WTG approximation on the intraseasonal time scale is of interest in future studies. Here, the convective instability mainly comes from moisture convergence. Whereas theoretical works (Wang 1988) and observation analysis (Hsu and Li 2012) all demonstrated the importance of moisture convergence in the MJO and in the boreal summer intraseasonal oscillation (Liu et al. 2015), other parts of convection is also important for the MJO; for example, the enhanced stratiform favors the good simulation of MJO in GCMs (Fu and Wang 2009), the upscale momentum and heat transfer from small to large scale may also play an important role in maintaining the MJO (Wang and Liu 2011; Liu et al. 2012; Liu and Wang 2012a, b, 2013a,, b), and other processes are reviewed by Zhang (2005). These processes should be also included in the future works.

Acknowledgments This study was supported by the National Basic Research Program of China (2015CB453200, 2012CB955604, and 2011CB309704), the National Outstanding Youth Science Fund Project of China (41425019), and the National Natural Science Foundation of China (41275083 and 91337105). This paper is the ESMC Contribution No. 0061.

References

Benedict JJ, Randall DA (2007) Observed characteristics of the MJO relative to maximum rainfall. J Atmos Sci 64:2332–2354

Del Genio AD, Chen Y, Kim D, Yao M-S (2012) The MJO transition from shallow to deep convection in CloudSat/CALIPSO data and GISS GCM simulations. J Clim 25:3755–3770

Fu X, Wang B (2009) Critical roles of the stratiform rainfall in sustaining the Madden-Julian oscillation: GCM experiments. J Clim 22:3939–3959

Hendon HH, Salby ML (1994) The life cycle of the Madden-Julian oscillation. J Atmos Sci 51:2225–2237

Hsu P-C, Li T (2012) Role of the boundary layer moisture asymmetry in causing the eastward propagation of the Madden-Julian oscillation. J Clim 25:4914–4931

Hsu P-C, Li T, Murakami H (2014) Moisture asymmetry and MJO eastward propagation in an aquaplanet general circulation model. J Clim 27:8747–8760

Jiang X, Waliser DE, Xavier PK, Petch J, Klingaman NP, Woolnough SJ, Guan B, Bellon G, Crueger T, DeMott C, Hannay C, Lin H, Hu W, Kim D, Lappen C-L, Lu M-M, Ma H-Y, Miyakawa T, Ridout JA, Schubert SD, Scinocca J, Seo K-H, Shindo E, Song X, Stan C, Tseng W-L, Wang W, Wu T, Wu X, Wyser K, Zhang GJ, Zhu AH (2015) Vertical structure and diabatic processes of the Madden-Julian oscillation: exploring key model physics in cimate simulations. J Geophys Res-Atmos in press

Kang I-S, Liu F, Ahn M-S, Yang Y-M, Wang B (2013) The role of SST structure in convectively coupled Kelvin–Rossby waves and its implications for MJO formation. J Clim 26:5915–5930

Khouider B, Majda AJ (2006) A simple multicloud parameterization for convectively coupled tropical waves. Part I: linear analysis. J Atmos Sci 63:1308–1323

Khouider B, Majda AJ (2007) A simple multicloud parameterization for convectively coupled tropical waves. Part II: nonlinear simulations. J Atmos Sci 64:381–400

Kiladis GN, Straub KH, Haertel PT (2005) Zonal and vertical structure of the Madden-Julian oscillation. J Atmos Sci 62:2790–2809

Kiladis GN, Wheeler MC, Haertel PT, Straub KH, Roundy PE (2009) Convectively coupled equatorial waves. Rev Geophys 47:2003

Knutson TR, Weickmann KM (1987) 30–60 day atmospheric oscillations: composite life cycles of convection and circulation anomalies. Mon Weather Rev 115:1407–1436

Liu F, Wang B (2012a) A frictional skeleton model for the Madden-Julian oscillation. J Atmos Sci 69:2749–2758

Liu F, Wang B (2012b) A model for the interaction between 2-day waves and moist Kelvin waves. J Atmos Sci 69:611–625

Liu F, Wang B (2013a) An air–sea coupled skeleton model for the Madden–Julian oscillation. J Atmos Sci 70:3147–3156

Liu F, Wang B (2013b) Impacts of upscale heat and momentum transfer by moist Kelvin waves on the Madden–Julian oscillation: a theoretical model study. Clim Dyn 40:213–224

Liu F, Huang G, Feng L (2012) Critical roles of convective momentum transfer in sustaining the multi-scale Madden–Julian oscillation. Theor Appl Climatol 108:471–477

Liu F, Huang G, Yan M (2014) Role of SST meridional structure in coupling the Kelvin and Rossby waves of the intraseasonal oscillation. Theor Appl Climatol. doi:10.1007/s00704-00014-01266-00700

Liu F, Wang B, Kang I-S (2015) Roles of barotropic convective momentum transport in the intraseasonal oscillation. J Clim 28:4908–4920

Madden RA, Julian PR (1971) Detection of a 40–50 day oscillation in the zonal wind in the tropical Pacific. J Atmos Sci 28:702–708

Madden RA, Julian PR (1972) Description of global-scale circulation cells in the tropics with a 40–50 day period. J Atmos Sci 29:1109–1123

Madden RA, Julian PR (1994) Observations of the 40–50-day tropical oscillation—a review. Mon Weather Rev 122:814–837

Majda AJ, Biello JA (2004) A multiscale model for tropical intraseasonal oscillations. Proc Natl Acad Sci U S A 101:4736–4741

Majda AJ, Stechmann SN (2009) The skeleton of tropical intraseasonal oscillations. Proc Natl Acad Sci U S A 106:8417–8422

Maloney ED, Hartmann DL (1998) Frictional moisture convergence in a composite life cycle of the Madden-Julian oscillation. J Clim 11:2387–2403

Mapes B, Tulich S, Lin J, Zuidema P (2006) The mesoscale convection life cycle: building block or prototype for large-scale tropical waves? Dyn Atmos Oceans 42:3–29

Mori M, Watanabe M (2008) The growth and triggering mechanisms of the PNA: a MJO-PNA coherence. J Meteorol Soc Jpn 86:213–236

Roundy PE (2008) Analysis of convectively coupled Kelvin waves in the Indian Ocean MJO. J Atmos Sci 65:1342–1359

Rui H, Wang B (1990) Development characteristics and dynamic structure of tropical intraseasonal convection anomalies. J Atmos Sci 47: 357–379

Salby ML, Hendon HH (1994) Intraseasonal behavior of clouds, temperature, and motion in the tropics. J Atmos Sci 51:2207–2224

Sobel A, Maloney E (2012) An idealized semi-empirical framework for modeling the Madden-Julian oscillation. J Atmos Sci 69:1691–1705

Sobel A, Maloney E (2013) Moisture modes and the eastward propagation of the MJO. J Atmos Sci 70:187–192

Sobel AH, Nilsson J, Polvani LM (2001) The weak temperature gradient approximation and balanced tropical moisture waves. J Atmos Sci 58:3650–3665

Wang B (1988) Dynamics of tropical low-frequency waves: an analysis of the moist Kelvin wave. J Atmos Sci 45:2051–2065

Wang B, Li T (1994) Convective interaction with boundary-layer dynamics in the development of a tropical intraseasonal system. J Atmos Sci 51:1386–1400

Wang B, Liu F (2011) A model for scale interaction in the Madden-Julian oscillation. J Atmos Sci 68:2524–2536

Wang B, Rui H (1990) Dynamics of the coupled moist Kelvin-Rossby wave on an equatorial β-plane. J Atmos Sci 47:397–413

Wheeler M, Kiladis GN (1999) Convectively coupled equatorial waves: analysis of clouds and temperature in the wavenumber-frequency domain. J Atmos Sci 56:374–399

Zhang C (2005) Madden-Julian Oscillation. Rev Geophys 43:RG2003. doi:10.1029/2004RG000158

Zhang GJ, Song X (2009) Interaction of deep and shallow convection is key to Madden-Julian oscillation simulation. Geophys Res Lett 36: 9708

Zhou S, Miller AJ (2005) The interaction of the Madden-Julian oscillation and the Arctic oscillation. J Clim 18:143–159